Single-cell analysis of mosquito hemocytes identifies signatures of immune cell sub-types and cell differentiation

Hyeogsun Kwon[1], Oscar Franzén[2], Mubasher Mohammed[3], Johan Ankarklev[3,4], Ryan C. Smith[1]*

[1]Department of Entomology, Iowa State University, Ames, Iowa, USA

[2]Integrated Cardio Metabolic Centre, Department of Medicine, Karolinska Institutet, Novum, 14157 Huddinge, Sweden

[3]Department of Molecular Biosciences, The Wenner-Gren Institute, Stockholm University, Stockholm, Sweden 10691

[4]Microbial Single Cell Genomics facility, SciLifeLab, Biomedical Center (BMC) Uppsala University, SE-751 23, Uppsala, Sweden

*Corresponding author: smithr@iastate.edu

Abstract

Mosquito immune cells, known as hemocytes, are integral to cellular and humoral responses that limit pathogen survival and mediate immune priming. However, without reliable cell markers and genetic tools, studies of mosquito immune cells have been limited to morphological observations, leaving several aspects of their biology uncharacterized. Here, we use single-cell RNA sequencing (scRNA-seq) to characterize mosquito immune cells, demonstrating an increased complexity to previously defined prohemocyte, oenocytoid, and granulocyte sub-types. Through functional assays relying on phagocytosis, phagocyte depletion, and RNA-FISH experiment, we define markers to accurately distinguish immune cell sub-types and provide evidence for immune cell maturation and differentiation. In addition, gene-silencing experiments demonstrate the importance of lozenge in defining the mosquito oenocytoid cell fate. Together, our scRNA-seq analysis provides an important foundation for studies of mosquito immune cell biology and a valuable resource for comparative invertebrate immunology.

Introduction

Across metazoa, immune cells are vital to promoting wound healing, maintaining homeostasis, and providing anti-pathogen defenses (Chaplin, 2010). With immune cells mediating both innate and adaptive immune function in vertebrates, immune cell sub-types display highly specialized roles that have continually been resolved by technological advancements that enable their study (Proserpio & Mahata, 2016; Papalexi & Satija, 2017). Recently, the advent of single-cell sequencing (scRNA-seq) has continued to delineate and provide further resolution into new cell types and immune cell functions in mammals (Amara Korba *et al*, 2016; Szabo *et al*, 2019). In lesser studied invertebrates lacking adaptive immunity, single-cell technologies have enhanced descriptions of previously described cell types and have redefined cell complexity (Severo *et al*, 2018; Cattenoz *et al*, 2020; Cho *et al*, 2020; Raddi *et al*, 2020; Tattikota *et al*, 2020).

In insects, hematopoiesis and immune cell function have predominantly been examined in Lepidoptera and *Drosophila* (Lavine & Strand, 2002; Banerjee *et al*, 2019), with the mosquito, *Anopheles gambiae*, recently serving as an emerging system of study (Kwon & Smith, 2019). However, the study of mosquito immune cells (or hemocytes) has been complicated by discrepancies in cell classification (Ribeiro & Brehélin, 2006), cell numbers (Hillyer & Strand, 2014), and methodologies to examine their function (Kwon & Smith, 2019). These constraints are magnified by the lack of genetic tools and markers that have limited studies of immune cells outside of *Drosophila* strictly to morphological properties of size and shape (Hillyer & Strand, 2014; Kwon & Smith, 2019).

Mosquito immune cell populations are integral to the cellular and humoral responses that limit invading pathogens in the mosquito host (Castillo *et al*, 2017; Smith *et al*, 2016; Kwon & Smith, 2019; Baton *et al*, 2009; Hillyer *et al*, 2003) and the establishment of immune memory (Rodrigues *et al*, 2010; Ramirez *et al*, 2015). Transcriptional (Pinto *et al*, 2009; Baton *et al*, 2009) and proteomic (Smith *et al*, 2016) analysis of mosquito hemocyte populations have yielded important information into the regulation of hemocyte function in response to blood-feeding and infection. Yet, the lack of genetic tools and markers has limited studies of mosquito immune cells to rely on unreliable morphological properties of size and shape.

Traditional classifications of mosquito hemocytes describe three cell types: prohemocyte precursors, phagocytic granulocytes, and oenocytoids that have primary roles in melanization (Castillo *et al*, 2006). However, recent studies have begun to challenge these immune cell classifications, demonstrating the existence of multiple types of phagocytic cells (Severo *et al*, 2018; Kwon & Smith, 2019) and that both granulocytes and oenocytoids are the source of prophenoloxidase expression (Severo *et al*, 2018; Kwon & Smith, 2019; Smith *et al*, 2016; Bryant & Michel, 2016). Together, this suggests that there is additional complexity to mosquito immune cells that is not accurately represented by the traditional classification of mosquito hemocytes into three cell types.

For this reason, here we employ the use of scRNA-seq to characterize mosquito immune cells. Using a conservative approach, we identify seven hemocyte sub-types with distinct molecular signatures and validate these characterizations using a variety of bioinformatic and experimental molecular techniques. We define new markers that can accurately distinguish immune cell sub-types, improving upon the ambiguity of existing methodologies. Moreover, our data supports a new model of immune cell differentiation and maturation that lead to a dynamic population of circulating immune cells in the adult female mosquito. In summary, these data represent a valuable resource to advance the study of mosquito immune cells and for comparative immunology, where our data support commonalities and distinct differences with other insect systems.

Results

Isolation of mosquito immune cells and scRNA-seq analysis

To examine mosquito immune cells by scRNA-seq, adult female *An. gambiae* were perfused as previously (Smith *et al*, 2015; Kwon *et al*, 2017; Kwon & Smith, 2019; Reynolds *et al*, 2020; Smith *et al*, 2016) from either naïve or blood-fed (24 h post-feeding) conditions to asses the physiological impacts of blood-feeding. Following perfusion, cells were stained with a live-dead viability stain to select for live cells, and FITC-conjugated wheat germ agglutinin (WGA) and DRAQ5 to label immune cells and nuclear content (Kwon & Smith, 2019) to separate cells by fluorescence-activated cell sorting (FACS) (Figure 1A). Based on distinct patterns in WGA/DRAQ5 intensity, cells were grouped into three “gates” to enrich for defined cell populations, while a non-selective fourth gate

isolated cells at random to estimate overall cell abundance (Figure 1A). Based on these parameters, individual cells were isolated by FACS into a 384-well plate for further processing for scRNA-seq using the SMART-seq2 methodology (Picelli *et al*, 2013, 2014). A total of 262 cells passed the quality filtering threshold of 10,000 reads per cell (Figure S1), yielding 194 and 68 cells, respectively from naïve and blood-fed conditions (Table S1). Overall, we detected expression (>0.1 RPKM) from ~46% (6352/13,764) of the *An. gambiae* genome, with a median of 1646 genes expressed per cell (range 45 to 5215). In comparison to Severo *et al.* (Severo *et al*, 2018), we see a comparable number of detected genes in our analysis. However, our data display a higher number of genes per cell and larger variance in genes between cell types, patterns suggestive of a broader range of cell populations represented in our data. All data can be visualized and searched using the following database link: https://alona.panglaodb.se/results.html?job=2c2r1NM5Zl2qcW44RSrjkHf3Oyv51y_5f09d74b770c9.

Using hierarchical clustering, we conservatively define eight distinct cell clusters or immune cell-subtypes (Figure 1B). These clusters are supported by the unique molecular profiles of each cell cluster when analyzed by tSNE (Figure 1C), as well as variability in the number of expressed genes (Figure 1D) that infers functional heterogeneity in these immune cell populations. When referenced to the FACS gating status (Figure 1A, Figure S2), each cell cluster is represented under non-selected gating (Gate 4), yet specific cell types display enrichment under each of the specific gating conditions (Gates 1-3; Figure S2). Clusters 1, 7, and 8 are enriched in Gate 1, Clusters 5 and 6 in Gate 2, and Clusters 2-4 in Gate 3 (Figure S2), arguing that these cells have similar physical properties in wheat germ agglutinin (WGA) staining and DNA content. With the exception of Cluster 3, which was only identified in naïve mosquitoes, each of the respective cell clusters were found under both naïve and blood-fed conditions (Figure S3). When paired with differential gene expression between naïve and blood-fed cells of each cluster, only Clusters 2 and 4 displayed significant changes in gene expression (Table S2). This suggests that blood-feeding may primarily influence the activation state and gene expression of specific immune cell sub-types as previously suggested (Reynolds *et al*, 2020; Smith *et al*, 2016).

Characterization of *An. gambiae* immune cell clusters

To further characterize the resulting cell clusters resulting from our scRNA-seq analysis, we examined a subset of genes to more closely define each of the eight putative immune cell clusters. *Nimrod B2* (AGAP029054) (Kwon & Smith, 2019; Severo *et al*, 2018; Estévez-Lao & Hillyer, 2014; Midega *et al*, 2013) and *SPARC* (AGAP000305) (Martinek *et al*, 2011; Cattenoz *et al*, 2020) were highly expressed in all cell clusters (Table S1, Figure 2A), and represent universal hemocyte markers. Unlike other cell clusters, Cluster 1 displayed high levels of gene expression for all genes examined (Figure 2A). When paired with its localization as an outlier in the t-SNE analysis (Figure 1C) and high median number of expressed genes (Figure 1D), we dismissed this cell cluster from further analysis as likely cell doublets of mixed cell origins as the result of FACS cell isolation or as dividing cells. Clusters 2-4 display similar patterns in gene expression and are highly enriched for several phagocytic marker genes: *LRIM15*, *SCRBQ2*, *SCRASP1*, *ninjurin*, and *LRIM16A* (Smith *et al*, 2016), indicating that Clusters 2-4 represent distinct populations of phagocytic granulocytes (Figure 2A). Cluster 5 exhibits lower levels of phagocytic genes, while displaying high levels of *ND1*, *ND2*, and *tRNA-Ser* that suggest a unique cellular function compared to other clusters (Figure 2A). Similar to Clusters 2-4, Cluster 6 displays similar, yet alternative patterns of phagocytic cell gene expression (Figure 2A). In contrast, Clusters 7 and 8 show distinctive patterns of *SCRB9*, *SCRB3*, *Gr9*, and *PPO1* gene expression that likely delineates oenocytoid cell populations (Figure 2A).

To more closely evaluate the molecular profiles of each cell cluster, transcripts identified in more than 80% of cells in each cluster (Table S3) were used to perform gene ontology (GO) analysis (Figure 2B). Comparisons across cell clusters provide further support that Clusters 2-4 are highly analogous in their core machinery, with Cluster 6 displaying a related, yet divergent cellular composition represented by an increased representation in translational machinery (Figure 2B). Cells in Cluster 5 display a unique profile predominantly comprised of genes implicated in redox metabolism/stress responses (Figure 2B), while Clusters 7 and 8 display marked differences in composition (Figure 2B), despite sharing similar markers to delineate these cell types (Figure 2A).

Comparisons with a previous study of the enriched phagocyte proteome in *An. gambiae* (Smith *et al*, 2016) demonstrate that transcripts of Clusters 2-4 have the strongest associations with phagocytic cell proteins (Figure S4), providing further support that these clusters represent populations of phagocytic granulocytes. Using average gene expression across cell clusters (Table S4), we examined the expression of mosquito orthologs of known *Drosophila* hemocyte genes (Waltzer *et al*, 2003; Fossett *et al*, 2003; Franc *et al*, 1996; Kocks *et al*, 2005; Dudzic *et al*, 2015; Stofanko *et al*, 2008; Manaka *et al*, 2004; Evans *et al*, 2014) to provide additional confirmation of our tentative cell cluster classifications (Figure 2C). Clusters 2-4 express the plasmatocyte (equivalent to mosquito granulocytes) markers *peroxinectin* (pxn), *croquemort* (crq), *eater*, and *Cg25C* (Figure 2C) suggestive of phagocytic cell function. In contrast, the expression of *lozenge* (lz) and *PPO1* indicative of *Drosophila* crystal cells (Tattikota *et al*, 2020; Evans *et al*, 2014; Cattenoz *et al*, 2020; Dudzic *et al*, 2015; Fossett *et al*, 2003) were most prevalent in Clusters 7 and 8 (Figure 2C), suggesting that these cell clusters are representative of oenocytoids cell populations (equivalent to *Drosophila* crystal cells). However, little resolution into the roles of Clusters 5 and 6 was provided through these comparisons to known *Drosophila* markers (Figure 2C).

Similar examinations of known mosquito hemocyte genes (Estévez-Lao & Hillyer, 2014; Severo *et al*, 2018; Kwon & Smith, 2019; Smith *et al*, 2016; Castillo *et al*, 2006; Danielli *et al*, 2000; Midega *et al*, 2013; Bryant & Michel, 2016; Pinto *et al*, 2009; Smith *et al*, 2015) were performed to provide additional resolution into our cell clusters (Figure 2D). Expression of the phagocytic markers, LRIM15, LRIM16A, and SCRASP1 (Smith *et al*, 2016) is highest in Clusters 2-4 (Figure 2D), while *Ninjirin* (Pinto *et al*, 2009) and *DOX-A2* (Castillo *et al*, 2006) in Clusters 2 and 4 can further delineate these presumed phagocytic cell types (Figure 2D). In addition, *AGAP007314* grouped strongly with the presumed oenocytoid cells of Cluster 8, supporting its previously described roles in melanization (Pinto *et al*, 2009). The patterns of *LysI* (AGAP011119) and *FBN10* (AGAP011230) used to respectively define $PPO6^{low}$ and $PPO6^{high}$ immune cell populations in previous scRNA-seq studies (Severo *et al*, 2018), also provide significant comparative insight into the immune cell populations defined in our study. We demonstrate that *LysI* is predominantly expressed in the likely phagocytic cells of Clusters 2-4, while *FBN10* can be found in both

tentative granulocyte and oenocytoid populations (Figure 2D, Figure S5). There is a significant correlation of *LysI* and *FBN10* with *PPO6* expression (Figure S5), mirroring the PPO6^{low} and PPO6^{high} phenotypes as previously described (Severo *et al*, 2018), yet our data argue that these cell markers do not accurately account for the added complexity of mosquito immune cell populations identified in our study.

When we examine the transcriptional profiles of prophenoloxidases (PPOs), a family of enzymes that catalyze the production of melanin in response to infection (Dudzic *et al*, 2015), we demonstrate that the eight PPOs detected in our analysis group into two distinct classes based on their expression patterns (Figure 2E). *PPO1*, *PPO3*, and *PPO8* are enriched in putative oenocytoids, while *PPO2*, *PPO4*, *PPO5*, *PPO6*, and *PPO9* are most abundant in putative granulocyte populations (Figure 2E). This is contrast with previous suggestions that PPOs are expressed in a subset of mosquito immune cells (Castillo *et al*, 2006; Hillyer & Strand, 2014) as in other insect systems (Dudzic *et al*, 2015), yet is supported by recent evidence that phagocytic granulocyte populations in mosquitoes also significantly contribute to *PPO* production (Smith *et al*, 2016; Kwon & Smith, 2019).

Additional characterizations of immune signaling pathways (Figure S6), SRPNs and CLIPs (Figure S7), chemosensory receptors/proteins (Figure S8), and tRNA expression (Figure S9) across cell clusters provide further detail into the functions of our tentative immune cell clusters. Known anti-microbial genes and signaling components of the Toll, IMD, and JAK-STAT pathways (Cirimotich *et al*, 2010) displayed the highest expression patterns in Clusters 2 and 8 (Figure S6), similar to the expression patterns of SRPNs and CLIPs (Figure S7) involved in the regulation of protease signaling cascades that mediate immune activation (Kanost & Jiang, 2015; Gulley *et al*, 2013). This suggests that these tentative granulocyte and oenocytoid populations respectively contribute to the expression of a distinct subset of immune signaling processes. However, it is unclear if this corresponds to pathogen-specific defenses or immune responses unique to each particular cell type. Interestingly, we noticed that the bulk of the receptors involved in chemosensory recognition (ionotropic, gustatory, and odorant receptors; odorant binding proteins) are highly expressed in Clusters 7 and 8 (Figure S8). Although their function has not been described in mosquitoes, the role of an odorant binding protein is essential

to the production of crystal cells (oenocytoids) in other insect systems (Benoit *et al*, 2017). Moreover, we also identified that the differential expression of transfer RNA (tRNA) genes provided useful measures to tease apart Clusters 5-8 from the other cell clusters (Figure S9) that may reflect different activation states or stages of immune cell development as previously defined in mammalian systems (Krishna *et al*, 2019; Torrent *et al*, 2018; Rak *et al*, 2020).

Based on these characterizations, our data support that Clusters 2-4 are likely phagocytic granulocytes, while Clusters 7 and 8 represent putative populations of oenocytoids (Figure 2F). However, Clusters 5 and 6 are less defined due to the lack of unique markers to distinguish these cell types (Figure 2). Cells of Cluster 6 are likely phagocytic, displaying properties unique from the other phagocytic cell populations, possibly representing a population of immature granulocytes (Figure 2F). Given the low number of expressed genes (Figure 1), the lack of discernable markers (Figure 2), and low levels of cyclin G2 (Table S4) that delineate differentiated cell populations (Martínez-Gac *et al*, 2004; Horne *et al*, 1997), we believe that Cluster 5 represents a progenitor population of mosquito immune cells loosely defined as prohemocytes (Figure 2F).

Confirmation of mosquito immune cell sub-types

To confirm the identification of our immune cell clusters and to establish a reliable set of markers to distinguish immune cell subtypes, we performed RNA-FISH on fixed immune cell populations and paired these observations with the phagocytic properties of each of the respective cell populations (Figure 3). As previously supported (Severo *et al*, 2018), we identified *Nimrod B2* (NimB2) as a “universal” marker expressed across cell clusters (Figure 3A). To serve as a marker for phagocytic cells, we demonstrate that *LRIM15* effectively labels phagocytic cell populations (Figure 3B), while the labeling of *SCRB9* (Figure 3C, Figure S10) and *SCRB3* denote mosquito oenocytoid populations (Figure S11). As further validation, RNA-FISH experiments performed with both *LRIM15* and *SCRB9* probes identify distinct populations of *LRIM15*$^{+}$ or *SCRB9*$^{+}$ cells, confirming that these markers label unique cell populations (Figure S12).

When these respective RNA-FISH markers are used to examine cell abundance, >90% of fixed cells are *NimB2*$^{+}$ (Figure 3D), further demonstrating its role as a reliable general

cell marker. *LRIM15*$^{+}$ phagocytic granulocyte populations represent ~60% of fixed cells, while only ~5% of cells are *SCRB9*$^{+}$ (Figure 3D). As expected, *LRIM15*$^{+}$ cells are highly phagocytic, while *SCRB9*$^{+}$ cells do not display phagocytic activity (Figure 3E), agreeing with the respective phagocytic and non-phagocytic roles of mosquito granulocytes and oenocytoids. Additional experiments using clodronate liposomes to deplete phagocytic cell populations (Kwon & Smith, 2019) demonstrate that *NimB2*$^{+}$/*LRIM15*$^{+}$ cells are highly susceptible to clodronate treatment (Figure 3F), providing further confirmation of their phagocytic cell function. The specificity of clodronate treatment was further validated by qRT-PCR, demonstrating that the expression of "universal" or "granulocyte" transcripts was reduced following phagocyte depletion, while "oenocytoid" markers remain unaffected (Figure 3E). Together, these data confirm the identification of our mosquito immune cell clusters and define the use of specific cell markers to delineate granulocyte and oenocytoid populations in *An. gambiae*.

However, ~30% of cells (most are *NimB2*$^{+}$) cannot be fully resolved by the expression of *LRIM15* and *SCRB9* alone (Figures 3B and 3C). This is evidenced by the *NimB2*$^{+}$/*LRIM15*$^{-}$ cells displayed in Figure 3F, which may represent other adherent cell populations with "granulocyte-like" morphology, potentially belonging to cells of Clusters 5 or 6 that are *LRIM15*$^{-}$ (Figure 3B).

Further definition of mosquito granulocyte and oenocytoid sub-populations

Based on the initial comparisons of known phagocytic cell markers (Figure 2) and the confirmation of phagocytic activity in *LRIM15*$^{+}$ cells (Figure 3), our data conservatively support the presence of four granulocyte sub-types (Clusters 2,3,4, and 6). To better define these sub-types, we more closely investigated the putative functional roles of each of these cell populations. Cells of Cluster 2 display high levels of immune gene expression of anti-microbial peptides (AMPs), components of the Toll pathway, *TEP1*, *MMP1*, and *LRIM26* (Figure S13) that may represent a class of specialized immune cells similar to other recent studies (Raddi *et al*, 2020; Tattikota *et al*, 2020; Cattenoz *et al*, 2020). However, tentative cell functions for the other cell clusters are less transparent. Cells of Cluster 3 have little immune gene expression and are distinguished by the increased production of *LRIM6*, *cathepsin L*, and *cathepsin F*, while cells in Cluster 4 display high

levels of *FBN 8*, *FBN 10*, and multiple PPO genes (Figure S13). By contrast, cells in Cluster 6 display reduced expression of several phagocytic markers (Figure S13), suggesting that cells of this sub-type lack the specialized phagocytic function of fully differentiated granulocytes. The reduced expression of *Cyclin G2* (Figure S13), a marker of differentiated cells (Horne *et al*, 1997; Martínez-Gac *et al*, 2004), supports this hypothesis. Together, these data support that Cluster 6 likely represents a granulocyte precursor, whereas Clusters 2-4 are differentiated sub-types with unique cell functions.

Similarly, differences in gene expression were also used to distinguish between the two oenocytoid sub-types. While both cell clusters express a subset of genes unique to the oenocytoid lineage (Figure 2), expression of most oenocytoid markers, such as *PPO1*, *SCRB3* and *SCRB9*, are higher in Cluster 8 (Figure S13). Moreover, Cluster 8 also expresses high levels of *hnt/peb*, *DnaJ-1*, *Mlf*, *klu*, and *lozenge* (Figure S13) that are indicative of mature *Drosophila* crystal cells (Koranteng *et al*, 2020; Terriente-Felix *et al*, 2013; Miller *et al*, 2017; Tattikota *et al*, 2020), suggesting that cells of Cluster 8 are mature oenocytoids while Cluster 7 represents a population of immature oenocytoids. This is further supported by the reduced expression of *Cyclin G2* in cells of Cluster 7 (Figure S13), characteristic of less differentiated cells (Horne *et al*, 1997; Martínez-Gac *et al*, 2004).

Differentiation of mosquito immune cell populations using lineage analysis

Previous studies in mosquitoes have suggested that prohemocyte precursors give rise into differentiated granulocyte and oenocytoid popoulations (Rodrigues *et al*, 2010; Ramirez *et al*, 2014; Smith *et al*, 2015), while additional evidence supports that granulocytes undergo mitosis to proliferate in response to infection (King & Hillyer, 2013). However, these observations have been based on morphological characterization, providing only speculation to the source of these immune cell populations. To better understand the origins of our identified immune cell clusters, we performed lineage analysis to determine relationships between the transcriptional profiles of individual cells to construct cell lineages in pseudotime using Monocle3 (Trapnell *et al*, 2014; Cao *et al*, 2019; Packer *et al*, 2019). Using marker genes for each respective cluster to root the analysis (Figure S14), individual cells were analyzed in pseudotime to reveal two distinct

lineages from a shared precursor population (Figure 4A). When visualized by cell cluster (Figure 4B), these patterns display that the presumed prohemocyte precursors of Cluster 5 serve as the initial branching point for our cell lineages delieneate into either granulocyte (Clusters 2, 3, 4, 6) or oenocytoid lineages (Clusters 7, 8). For the granulocyte lineage, precursor cells progress into cells of Cluster 6, then Cluster 4 before final maturation in the specialized cell populations of Cluster 2 and Cluster 3 (Figure 4B). In contrast, for the oenocytoid lineage, precursor cells differentiate into cells from Clusters 7 and 8 (Figure B). Based on these cell trajectories (Figures 4A and 4B) and transcriptional differences that likely define immature cell types (Figure S13), we summarized our results into a model for immune cell differentiation and the progression of cells within each lineage (Figure 4C). Moreover, using features of Monocle3 analysis, we define distinct subsets of genes that define cell populations in their cell lineage trajectories (Figure S15, Table S5). Together, these data confirm the differentiation of cells from a prohemocyte precursor as previously proposed (Rodrigues *et al*, 2010; Ramirez *et al*, 2014; Smith *et al*, 2015), yet also provide new insight into the potential role of intermediate cell types before terminal differentiation of immune cell sub-types (Figure 4C) similar to those recently described in *Drosophila* (Tattikota *et al*, 2020).

Lozenge promotes differentiation of the oenocytoid lineage

While several genes have been described that promote *Drosophila* immune cell lineages (Evans *et al*, 2014), the factors that define mosquito immune cell lineages have not been described beyond the role of multiple immune signaling pathways that influence hemocyte differentiation in response to malaria parasite infection (Ramirez *et al*, 2014; Smith *et al*, 2015). To further explore the factors that determine mosquito immune cell lineages, we focused on oenocytoid differentiation and the role of lozenge. In *Drosophila*, *lozenge* (lz) expression is integral to defining crystal cell fate (Waltzer *et al*, 2003; Fossett *et al*, 2003), the equivalent of mosquito oenocytoids. To similarly examine the role of lozenge in mosquito oenocytoid development, we used RNA-FISH to demonstrate and confirm the expression of *lozenge* in mosquito immune cells (Figure 5A). *Lozenge* was detected in ~15% of fixed cells (Figure 5B), a much higher percentage than that of *SCRB9*$^{+}$ cells demarcating *An. gambiae* oenocytoids (Figure 3). When we more closely examined the expression of *lozenge* and *SCRB9*, we see that co-localization of both markers only

occurs in a subset of *lozenge*$^{+}$ cells (Figure 5C), suggesting that *lozenge* is expressed in other immune cell sub-types in addition to mosquito oenocytoid populations. This is supported by the expression of *lozenge* in other immune cell clusters (Figure 5A), the ability of a subset of lozenge+ cells to undergo phagocytosis, and the depletion of lozenge+ cells and lozenge expression following depletion of phagocytic cell populations (Figure S16). To evaluate the influence of *lozenge* on oenocytoid cell fate, we silenced *lozenge* expression by RNAi (Figure S17), and examined the co-localization of *LRIM15/SCRB9* by RNA-FISH. In *lz*-silenced mosquitoes, we see a significant decrease in *LRIM15*$^{-}$*/SCRB9*$^{+}$ cells (Figure 5D), suggesting that *lozenge* is integral to defining the oenocytoid lineage. This is further supported by the specific reduction of *PPO1/3/8* expression (Figure 5E), PPOs that are enriched in Clusters 7 and 8 corresponding to the oenocytoid cell fate (Figure 2E). Together, these data support that *lozenge* expression is an important driver of the oenocytoid lineage in *An. gambiae* (Figure 5F). Based on our cell trajectories proposed in Figure 4, it suggests lozenge^{+} prohemocytes promote the differentiation into an oenocytoid. However, the presence of *lozenge* in a subset of phagocytic granulocyte populations (Figure 5, Figure S16) alternatively supports a model of transdifferentiation in which oenocytoids can be derived form phagocytic granulocytes as previously proposed in *Drosophila* (Leitao & Sucena, 2015).

Discussion

Our understanding of mosquito immune cells has largely been shaped by studies in other insects (Lavine & Strand, 2002; Banerjee *et al*, 2019). From morphological observations of size and shape, three cell types have been described in mosquitoes: prohemocytes, oenocytoids, and granulocytes (Castillo *et al*, 2006). However, with the advent of additional molecular tools to study mosquito immune cell function, several studies have supported an increased complexity of hemocyte populations beyond these generalized cell sub-type classifications (Smith *et al*, 2016; Bryant & Michel, 2016; Severo *et al*, 2018; Kwon & Smith, 2019; Pondeville *et al*, 2020; Raddi *et al*, 2020). Herein, we demonstrate through scRNA-seq experiments and additional molecular characterization, that there are at least seven conservatively defined immune cell populations in *An. gambiae*.

Similar to previous characterizations (Castillo *et al*, 2006), we identify prohemocyte, oenocytoid, and granulocyte populations in our RNA-seq analysis. However, in both the oenocytoid and granulocyte classifications, we identify multiple, distinct immune cell populations defined by developmental progression, activation state, or specialized immune function similar to those recently described in *Drosophila* (Tattikota *et al*, 2020; Cattenoz *et al*, 2020). Moreover, we provide an initial set of markers to accurately distinguish between mosquito immune cell populations using RNA-FISH, and validate these identifications through co-localization experiments, phagocytosis experiments, and phagocyte depletion assays. Therefore, these experiments provide important and much-needed cell markers that reliably distinguish oenocytoid and granulocyte populations to advance the study of mosquito immune cells.

Through our scRNA-seq analysis, we identify at least four granulocyte sub-types in *An. gambiae* based on gene expression, previous proteomics studies (Smith *et al*, 2016), and phagocytic properties. This expansion of the general "granulocyte" classification is supported by previous morphological observations of granulocytes in mosquitoes (Kwon & Smith, 2019; Pondeville *et al*, 2020), and more recently by parallel scRNA-seq experiments in *Drosophila* (Tattikota *et al*, 2020; Cattenoz *et al*, 2020) and *An. gambiae* (Raddi *et al*, 2020). Of these four granulocyte sub-types, our data support that cells of Cluster 6 are intermediate or immature granulocyte forms that display distinct expression patterns from prohemocyte precursors, yet do not have the same properties of other granulocyte sub-types (Cluster 2-4). This is supported by our pseudotime lineage analysis, where these immature cells of Cluster 6 give rise to more specialized granulocyte populations, similar to that described for comparable immature plasmatocytes in *Drosophila* (Tattikota *et al*, 2020). This maturation includes the increased expression of the phagocytic cell markers *LRIM15*, *LRIM16A*, and *SCRASP1* (Smith *et al*, 2016) and the differentiated cell marker Cyclin G2 (Horne *et al*, 1997; Martínez-Gac *et al*, 2004), resulting in the maturation of more specialized granulocyte sub-types (Clusters 2-4).

Cells of Cluster 4 display high levels of *PPO2/4/6* expression distinct from other granulocyte sub-types, and therefore can likely be attributed to the reduction of

phenoloxidase (PO) activity following phagocyte depletion in experiments with clodronate liposomes (Kwon & Smith, 2019). Granulocytes of Cluster 4 also display high levels of *FBN10*, which closely resemble previously described PPO6^{high} phagocytic cell populations (Severo *et al*, 2018; Kwon & Smith, 2019). Based on our lineage analysis, Cluster 4 may serve as an additional intermediate, giving rise to cells of Clusters 2 and 3, or alternatively represent different activation states. In support of this, Cluster 3 cells were only identified under naïve conditions, whereas both Clusters 2 and 4 displayed transcriptional changes in response to blood-feeding.

Cluster 3 granulocytes are delineated by the expression of *LRIM6*, as well as *cathepsin L* and *cathepsin F*. In other invertebrate systems, cathepsin L has been implicated in hemocyte lysosomes, serving important roles in the degradation of phagocytosed materials by phagocytic immune cells (Tryselius & Hultmark, 1997; Jiang *et al*, 2018), with both cathepsin L and cathepsin F associated with anti-microbial activity (Jiang *et al*, 2018; Guo *et al*, 2018). Therefore, the phagocytic granulocytes of Cluster 3 likely play an important role in immunity and homeostasis, although at present it is unclear why these cells are only detected under naïve conditions.

The remaining granulocyte cell type, Cluster 2, display increased immune properties reminiscent of other granulocyte or comparable plasmatocyte populations recently described in respective scRNA-seq studies in *An. gambiae* (Raddi *et al*, 2020) or *Drosophila* (Tattikota *et al*, 2020; Cattenoz *et al*, 2020). Cells of Cluster 2 display increased levels of the anti-microbial peptides (AMPs) *attacin*, *DEF1*, *CEC3*, and *gambicin* (GAM1), as well as the immune components *REL2* and *TEP1.* This suggests that these cell populations have an integral role in the hemocyte-mediated humoral immune responses that limit invading pathogens.

In addition, we also define two populations of mosquito oenocytoids (clusters 7 and 8) that likely reflect immature and mature cell populations similar to orthologous crystal cell populations described in *Drosophila* (Tattikota *et al*, 2020; Cho *et al*, 2020; Koranteng *et al*, 2020). The mature oenocytoids of Cluster 8 are denoted in part by the increased expression of *lozenge*, *PPO1*, *pebbled*, *DNA J*, *MLF*, *Notch*, and *klumpfuss* as previously described (Tattikota *et al*, 2020; Cho *et al*, 2020; Koranteng *et al*, 2020), as well as the

increase in *SCRB3* and *SCRB9* which serve as a new marker of mosquito oenocytoids in our analysis. Despite these differences in cell maturation, the mosquito oenocytoid lineage is distinct from that of granulocytes and relies on the expression of *lozenge* to promote oenocytoid differentiation similar to its role in *Drosophila* crystal cells (Fossett *et al*, 2003; Waltzer *et al*, 2003). Based on our analysis, this differentiation likely occurs from circulating prohemocyte precursor populations (Cluster 5), yet we cannot rule out the potential that immature granulocyte populations are able to undergo transdifferentiation as previously described in *Drosophila* (Leitao & Sucena, 2015). Moreover, our ability to accurately identify oenocytoid populations by RNA-FISH demonstrates that mosquito oenocytoid populations are not phagocytic, which contrasts previous reports of rare phagocytic events by oenocytoids when relying only on cellular morphology (Hillyer *et al*, 2003).

Traditionally, insect oenocytoids/crystal cells have been primarily associated with prophenoloxidase (PPO) production and melanization (Lavine & Strand, 2002; Lu *et al*, 2014; Hillyer & Strand, 2014). Much of this stems from work in *Drosophila*, where two of the three PPOs (*PPO1* and *PPO2)* are expressed in crystal cells (Dudzic *et al*, 2015), and in *Bombyx mori* where PPO is synthesized exclusively by oenocytoids (Iwama & Ashida, 1986). However, our scRNA-seq results suggest that both granulocytes and oenocytoids are involved in PPO production. Moreover, through clustering analysis and the effects of *lozenge*-silencing, our data support that distinct subsets of PPOs are differentially regulated in the granulocyte and oenocytoid lineages. The expression of PPOs in *An. gambiae* granulocytes populations is further supported by previous studies examining PPO6 transgene expression and staining in mosquito granulocytes (Severo *et al*, 2018; Castillo *et al*, 2006; Bryant & Michel, 2014, 2016; Kwon & Smith, 2019), the effects of phagocyte depletion on PPO expression (Kwon & Smith, 2019), and the identification of multiple PPOs in the mosquito phagocyte proteome (Smith *et al*, 2016). This departure from other insect systems is most likely a reflection of the expansion of the PPO gene family in mosquito species, where a total of 9 *An. gambiae* PPOs have been annotated with yet undescribed function. Together, these results suggest new possible roles for PPOs in mosquito immune cells and their respective roles in the innate immune response.

Initial comparisons to recently published *Drosophila* immune cell scRNA-seq experiments (Cattenoz *et al*, 2020; Tattikota *et al*, 2020) reveal both similarities and differences in immune cell populations between dipteran species. Similar to *Drosophila*, our data in mosquitoes support the developmental progression and specialization of immune cells from precursor populations, the presence of multiple phagocytic cell populations, and multiple shared markers that delineate the oenocytoid/crystal cell lineage (Cattenoz *et al*, 2020; Tattikota *et al*, 2020). However, several differences are also noted in mosquitoes, including the absence of well-characterized *Drosophila* immune cell markers such as hemolectin (Goto *et al*, 2003; Pondeville *et al*, 2020) and hemese (Kurucz *et al*, 2003), and the lack of lamellocyte cell populations. We also identify several mosquito immune cell markers, such as LRIM15 and the expansion of PPO genes, which are unique to mosquito immune cell populations. Other respective differences in the isolation of cells from larvae or adults in *Drosophila* and mosquitoes, may further explain other disparities in cell types or steady states of activation. Ultimately, these questions require a more in-depth comparison of immune cells between these two species in the future.

When placed in the context of previously published scRNA-seq studies in mosquitoes (Severo *et al*, 2018), our results build upon this previous advancement. From this initial characterization of 25 cells and classification of two immune cell sub-types, $PPO6^{high}$ and $PPO6^{low}$ (Severo *et al*, 2018), we have increased the number of cells examined (to 262), expanded upon the number of characterized immune cell sub-types, and validated the progression of the granulocyte and oenocytoid lineages from prohemocyte precursors. Moreover, we provide a reliable set of lineage-specific markers that aid in the identification of mosquito immune cells, that when paired with recent methods of phagocyte depletion (Kwon & Smith, 2019), provide an enhanced set of tools to define mosquito immune cell populations. From our experiments, we provide support based on phagocytic ability and homology of their gene expression profiles, the previously defined $PPO6^{high}$ and $PPO6^{low}$ populations (Severo *et al*, 2018) are representative of distinct granulocyte sub-types identified in our analysis. Therefore, our results improve upon existing data to increase the consistency and resolution in the study of mosquito immune cells.

In summary, our characterization of mosquito hemocytes by scRNA-seq provides an important advancement in our understanding of *An. gambiae* immune cell populations. Through the molecular characterization of at least seven immune cell subtypes and the development of dependable molecular markers to distinguish between cell lineages, we have developed new molecular tools where genetic resources were previously lacking. While serving as an important resource for the vector community, our data offer new insights into the complexity of mosquito immune cells that will provide a strong foundation for comparative function of insect immune cells.

Materials and Methods

Mosquito rearing

Adult *An*. *gambiae* mosquitoes of the Keele strain (Hurd *et al*, 2005; Ranford-Cartwright *et al*, 2016) were reared at 27°C with 80% relative humidity and a 14/10 hour light/dark cycle. Larvae were reared on a diet of fish flakes (Tetramin, Tetra), while adult mosquitoes were maintained on 10% sucrose solution and commercial sheep blood for egg production.

Isolation and sorting of mosquito immune cells for single-cell RNA sequencing

Hemolymph was perfused from female mosquitoes (n=40) under naïve (3- to 5-day old) or blood-fed (~24h post-feeding) conditions using an anticoagulant solution as previously described (Smith *et al*, 2016; Kwon & Smith, 2019). Perfused hemolymph was diluted with 1X PBS to a total volume of 1 mL, then centrifuged for 5 min at 2000×g to pellet cells. After the supernatant was discarded, cells were washed two times in 1X PBS with an additional centrifugation step of 5 min at 2000×g between washing steps. Cells were incubated with WGA (1:5000, Sigma), DRAQ5 (1:1000, Thermo Fisher Scientific) and Live/Dead Fixable Dead Cell Stain (1:1000 Thermo Fisher Scientific) for 90 min at room temperature. Following incubation, cells were washed twice in 1X PBS to remove excess stain with a centrifugation step of 5 min at 2000 ×g and run on a BD FACSCanto cytometer (BD Biosciences). Based on the previous flow cytometry data for establishment of threshold values for gating (Kwon & Smith, 2019), cells smaller or larger than single cells were excluded. Cell viability was determined by the intensity of the blue fluorescent signal from the Live/Dead Fixable Dead Cell Stain, where dead cells display higher fluorescent

signal. Following gating for cell viability, cell populations were distinguished by WGA and DRAQ5 signals and with individual cells sorted into each well of a 384-well plate (twintec^{TM} PCR plates, Eppendorf, Germany) containing 2.3 µl lysis buffer (Picelli *et al*, 2013).

cDNA libraries were generated using a slightly modified version of Smart-seq2 as previously described (Picelli *et al*, 2013), where 23 cycles for cDNA amplification were used. Single-cell libraries were sequenced on the HiSeq2500 platform (Illumina) using 56 base pair single-end sequencing. Library preparation and sequencing was performed at ESCG and NGI, SciLifeLab, Sweden..

Computational analysis

Sequencing reads were mapped to the *Anopheles gambiae* AgamP4 reference genome (Ensembl release 40) and ERCC sequences with the HISAT2 aligner version 2.1.0 (Kim *et al*, 2015). Only alignments with mapping quality 60 were retained. Quantification of gene expression was performed on the gene level. Overlapping exons of the same gene were merged based on their annotation coordinates. Counting of alignments on genome annotations was performed with the program subread version 1.6.2 (Liao *et al*, 2014) with the '-s' flag set to 0. Quality control of the data was performed by examining the fraction of sequencing output from ERCC templates versus the genome. Moreover, we applied a threshold of minimum 10,000 uniquely mapped reads per cell, only considering reads mapped in exons, i.e. intronic and intergenic reads are not counted towards the 10,000-minimum threshold; cells with fewer reads were not included in downstream analyses. Raw read counts were normalized to RPKM to adjust for gene length (Mortazavi *et al*, 2008). RPKM values were transformed with the function log2(**x**+1), where **x** is a vector of expression values. The complete quality-filtered gene expression data (as RPKM values) for all 262 cells is found in Table S1. Statistical analyses and data visualization were performed with the R software (www.r-project.org) version 3.5.3. Hierarchical clustering with Euclidean distance was used to define cell clusters; the ward.D2 agglomeration method was used for linkage. The final clusters were defined using a combination of manual examination of the tree structure and the cutreeDynamic function of the R package dynamicTreeCut (with method set to hybrid and deepSplit set to 4) (Langfelder

et al, 2008). Other clustering methods such as k-means clustering was explored but not found suitable.

Clustering and functional analysis of single-cell data

Raw reads count for single cells data were scaled and normalized using scale factor function (log10) for genes of interest. The percentage and the average expression of the selected genes were calculated in a scaled normalized expression along continuous color scale. Seurat Dotplot version (3.1.5) was used for visualization in R (version 3.5.3) software. The color intensity is proportional to a scaled average gene expression level for the selected genes across all clusters and the size of the circle is correspondence to the percentage of cells within cluster expressing a gene (Stuart & Satija, 2019).

Heatmaps were produced using the pheatmap package (version 1.0.12), where the average expression of the selected genes was calculated from the normalized scaled RPKM values from clustering data. The working data frame matrix was prepared using tidy-verse package version (1.3.0) for heatmap construction on selected gene sets corresponding (hemocyte gene orthologs, immune genes, etc.) to visualize expression across clusters. The clustering distance applied to the heatmaps was based on spearman.complete.obs with the scale set to be the selected genes as comparison for visualization. Color intensity corresponds to the average transcript abundance encoded with navy, white, red and firebrick 3, with the latter indicating a significant increase in the expression of a given gene.

To perform gene ontology (GO) analysis on each of the defined cell clusters, transcripts expressed in >80% of each respective cell cluster (Table S3) were examined to characterize the molecular composition of each cell type. Gene IDs (AGAP accession numbers) were classified based on gene ontology as previously (Smith *et al*, 2016; Mendes *et al*, 2011) to identify the functional categories of proteins within each cell cluster and to enable comparisons between cell clusters.

Differential expression analysis was performed using linear models as implemented in the alona software (https://github.com/oscar-franzen/alona/) (Franzén & Björkegren, 2020). Genes with false discovery rate (FDR; Benjamini-Hochberg's procedure) <5% and the absolute value of the log fold change>1.5 were considered significantly differentially

expressed. All data can be visualized using the alona server (Franzén & Björkegren, 2020) at the following project link: https://alona.panglaodb.se/results.html?job=2c2r1NM5Zl2qcW44RSrjkHf3Oyv51y_5f09d74b770c9.

Cell trajectory and pseudotime analysis

Cells were assigned to cell groups using Monocle3 with UMAP clustering (Trapnell *et al*, 2014; Qiu *et al*, 2017b; Cao *et al*, 2019; Packer *et al*, 2019). Data was normalized to remove batch effects using PCA clustering to 100 dimensions (Haghverdi *et al*, 2018). Pseudotime was calculated in Monocle3, with colors representing pseudotime changes among the cell clusters (Trapnell *et al*, 2014; Cao *et al*, 2019; Packer *et al*, 2019; Qiu *et al*, 2017b). The top 3 marker genes expressed in each cluster were plotted with at least 10% of cells expressing the respective genes, using 10 cells as reference (Qiu *et al*, 2017a). Bioinformatic methods for Monocle analyses can be found at: https://github.com/ISUgenomics/SingleCellRNAseq_RyanSmith.

RNA-FISH

In order to classify hemocyte populations by detecting specific RNA expression, we used RNAscope®Multiplex Fluorescent Reagent Kit v2 Assay (Advanced Cell Diagnostics), and *in situ* hybrization was performed using manufacturer's instruction. Using anticoagulant solution, hemolymph perfused from non-blood fed mosquitoes at 3- to 5-day old was placed on a superfrost microscopic slide (Fisher Scientific) and allowed to adhere at RT for 20 min. Cells were fixed with 4% paraformaldehyde for 15 min at 4°C, then washed three times with 1X PBS. Hydrogen peroxide was applied to the cells and slides were incubated for 10 min at room temperature (RT). After washed three times in sterile distilled water, cells were treated Protease IV and incubated for 30 min at RT. To delineate hemocyte populations, nimrod B2 (AGAP029054) RNA probe conjugated with C1 was use as a universal maker which was mixed with a specific RNA probe conjugated with C2 of either leucine rich-repeat immune protein 15 (LRIM15: AGAP007045) or lozenge (Lz: AGAP002506). In addition, Class B scavenger receptor, SCRB3 (AGAP005725) or SCRB9 (AGAP004846) RNA probe conjugated with C1 was prepared for identification of oenocytoid populations. The respective SCRB probe was co-incubated

with either LRIM15 or Lz probe. Hemocytes were hybridized with the mixture RNA probes in HybEZ™Oven for 2 h at 40°C. After washed two times with wash buffer for 2 min, hybridized probes were incubated with respective AMP reagents (AMP1 and AMP2) for 30 min at 40°C and with AMP3 for 15 min at 40°C. Cells were washed two times with wash buffer between AMP incubations. Cells were incubated with RNAscope®Multiplex FLv2 HRP-C1 for 15 min at 40°C, labeled with selected Opal Fluorophore reagent (Akoya Bioscience) at dilution facto (1:1000) for 30 min at 40°C and treated with RNAscope®Multiplex FLv2 HRP blocker for 15 min at 40°C. Cells were washed two times with wash buffer for 2 min between incubations. Following C1 labelling, cells were incubated with a specific RNAscope®Multiplex FLv2 HRP-C2 conjugated solution, desired Opal Fluorophore reagent (1:1000; Opal™520 or Opal™570) and HRP blocker. Slides were initially treated DAPI (Advanced Cell Diagnostics) for 30 sec at RT and mounted with ProLong®Diamond Antifade Mountant with DAPI (Life Technologies). Cells displaying a positive signal were quantified as the percentage of positive cells of the total number of cells examined. Counts were performed from >50 adherent cells per mosquito from randomly chosen fields using fluorescence microscopy (Nikon Eclipse 50i, Nikon).

Phagocytosis assays

Phagocytosis assays were performed by injecting 69 nl of 2% green fluorescent FluoSpheres (vol/vol) in 1X PBS to naïve female mosquitoes (3- to 5-day old) using a Nanoject II injector (Drummond Scientific). After injection, mosquitoes were kept at 27°C for 2 h, and hemolymph was perfused on a superfrost microscopic slide. To define phagocytic cell populations, phagocytosis assays were paired with RNA-FISH experiments as described above using *LRIM15*, *SCRB9*, and *Lz* RNA probes. The proportion of phagocytic cells was quantified as the number of cells that had uptaken one or more beads while displaying a positive signal for each of the respective RNA-FISH probes of the total number of cells examined. Counts were performed from >50 adherent cells per mosquito from randomly chosen fields using fluorescence microscopy (Nikon Eclipse 50i, Nikon).

Phagocyte depletion using clodronate liposomes

To confirm the identification of phagocytic cells in our cell clusters, validation experiments were performed using clodronate liposomes (CLD) to deplete phagocytic hemocytes (Kwon & Smith, 2019). Naïve female mosquitoes (3- to 5-day old) were injected with either 69 nl of control liposomes (LP) or CLD (Standard macrophage depletion kit, Encapsula NanoSciences LLC) at 1:5 dilution in 1X PBS. At 24 h post-injection, hemolymph was perfused, and RNA-FISH was performed to differentiate affected cells populations using RNA probes for NimB2 (C1), LRIM15 (C2), and Lz (C2) as described above. Hemocytes displaying a positive signal were quantified from 50 or more cells per mosquito.

qRT-PCR

Gene expression analysis using qRT-PCR was performed to validate the influence of phagocyte depletion on non-phagocytic and phagocytic cells. cDNA was prepared from the previous studies (Kwon & Smith, 2019) corresponding to naïve adult female *An. gambiae* treated with either control liposomes (LP) or clodronate liposomes (CLD) 24 h post-treatment. Hemocyte cDNA was prepared as previously described (Kwon & Smith, 2019) to analyze relative gene expression of *lozenge* between LP and CLD treatments. Specific transcripts representative of non-phagocytic and phagocytic cell populations were examined by qRT-PCR using primers listed in Table S6.

Gene silencing by RNAi

RNAi experiments were performed as previously described (Kwon & Smith, 2019; Smith *et al*, 2015, 2016; Kwon *et al*, 2017; Reynolds *et al*, 2020). T7 primers for lozenge (Lz; AGAP002506) were designed using the E-RNAi web application (http://www.dkfz.de/signaling/e-rnai3/idseq.php) and listed in Table S7. T7 templates for dsRNA synthesis were prepared from amplified cDNA from 4-day old whole naïve mosquitoes. PCR amplicons were purified using the DNA Clean & Concentration kit (Zymo Research), and dsRNAs were synthesized using the MEGAscript RNAi kit (Life Technologies). Subsequent dsRNA targeting GFP (control) or Lz was resuspended in nuclease free water to 3 µg/µl after ethanol precipitation. Injections were performed in three- to four-day old cold anesthetized mosquitoes by intrathoracic injection with 69 nl (~200 ng) of dsRNA per mosquito using a Nanoject III . The effects of gene silencing were measured at 3 days post-injection in whole mosquitoes (n=15) by qRT-PCR as previously

described (Kwon & Smith, 2019; Smith *et al*, 2015, 2016; Kwon *et al*, 2017; Reynolds *et al*, 2020).

Acknowledgements

We would like to thank Shawn Rigby of the Iowa State Flow Cytometry Facilty for his assistance with FACS, the Eukaryotic Single Cell Genomics (ESCG) facility, SciLifeLab, for assistance with single-cell library preparation and The National Genomics Infrastructure, SciLifeLab, Sweden for assistance with Illumina sequencing. Maiara Severo-Witte and Elena Levashina for initial assistance with the RNA-FISH methods, as well as Rick Masonbrink and Andrew Severin of the Iowa State Genome Informatics Facility for assistance with the single-cell RNA-seq analysis. This work was supported by the Swedish Society for Medical Research (SSMF) and the Swedish Research Council (VR-NT) to J.A., the Agricultural Experiment Station at Iowa State University and the National Institutes of Health, National Institute of Allergy and Infectious Diseases (R21 AI44705) to R.C.S.

References

Amara Korba R, Alayat MS, Bouiba L, Boudrissa A, Bouslama Z, Boukraa S, Francis F, Failloux A-B, Boubidi SC, Vinogradova E, Meegan J, Khalil G, Hoogstraal H, Adham F, Moutailler S, Krida G, Schaffner F, Vazeille M, Failloux A, Krida G, et al (2016) Ecological differentiation of members of the Culex pipiens complex, potential vectors of West Nile virus and Rift Valley fever virus in Algeria. *Parasit. Vectors* **9:** 455

Banerjee U, Girard JR, Goins LM & Spratford CM (2019) Drosophila as a genetic model for hematopoiesis. *Genetics* **211:** 367–417

Baton LA, Robertson A, Warr E, Strand MR & Dimopoulos G (2009) Genome-wide transcriptomic profiling of Anopheles gambiae hemocytes reveals pathogen-specific signatures upon bacterial challenge and Plasmodium berghei infection. *BMC Genomics* **10:** 257

Benoit JB, Vigneron A, Broderick NA, Wu Y, Sun JS, Carlson JR, Aksoy S & Weiss BL (2017) Symbiont-induced odorant binding proteins mediate insect host hematopoiesis. *Elife* **6:** 709–719

Bryant WB & Michel K (2014) Blood feeding induces hemocyte proliferation and activation in the African malaria mosquito, Anopheles gambiae Giles. *J. Exp. Biol.* **217:** 1238–45

Bryant WB & Michel K (2016) Anopheles gambiae hemocytes exhibit transient states of activation. *Dev. Comp. Immunol.* **55:** 119–129

Cao J, Spielmann M, Qiu X, Huang X, Ibrahim DM, Hill AJ, Zhang F, Mundlos S, Christiansen L, Steemers FJ, Trapnell C & Shendure J (2019) The single-cell transcriptional landscape of mammalian organogenesis. *Nature* **566:** 496–502

Castillo JC, Beatriz A, Ferreira B, Trisnadi N & Barillas-mury C (2017) Activation of mosquito complement antiplasmodial response requires cellular immunity. *Sci. Immunol.* **2:** eaal1505

Castillo JC, Robertson AE & Strand MR (2006) Characterization of hemocytes from the mosquitoes Anopheles gambiae and Aedes aegypti. *Insect Biochem. Mol. Biol.* **36:**

891–903

Cattenoz PB, Sakr R, Pavlidaki A, Delaporte C, Riba A, Molina N, Hariharan N, Mukherjee T & Giangrande A (2020) Temporal specificity and heterogeneity of Drosophila immune cells . *EMBO J.***:** 1–25

Chaplin DD (2010) Overview of the immune response. *J. Allergy Clin. Immunol.* **125:** S3–S23

Cho B, Yoon S-H, Lee D, Koranteng F, Tattikota SG, Cha N, Shin M, Do H, Hu Y, Oh SY, Moon SJ, Perrimon N, Nam J-W & Shim J (2020) Single-cell transcriptome maps of myeloid blood cell lineages in Drosophila. *bioRxiv***:** 2020.01.15.908350

Cirimotich CM, Dong Y, Garver LS, Sim S & Dimopoulos G (2010) Mosquito immune defenses against Plasmodium infection. *Dev. Comp. Immunol.* **34:** 387–395

Danielli a, Loukeris TG, Lagueux M, Müller HM, Richman a & Kafatos FC (2000) A modular chitin-binding protease associated with hemocytes and hemolymph in the mosquito Anopheles gambiae. *Proc. Natl. Acad. Sci. U. S. A.* **97:** 7136–7141

Dudzic JP, Kondo S, Ueda R, Bergman CM & Lemaitre B (2015) Drosophila innate immunity: Regional and functional specialization of prophenoloxidases. *BMC Biol.* **13:** 1–16

Estévez-Lao TY & Hillyer JF (2014) Involvement of the Anopheles gambiae Nimrod gene family in mosquito immune responses. *Insect Biochem. Mol. Biol.* **44:** 12–22

Evans CJ, Liu T & Banerjee U (2014) Drosophila hematopoiesis: Markers and methods for molecular genetic analysis. *Methods* **68:** 242–251

Fossett N, Hyman K, Gajewski K, Orkin SH & Schulz R a (2003) Combinatorial interactions of serpent, lozenge, and U-shaped regulate crystal cell lineage commitment during Drosophila hematopoiesis. *Proc. Natl. Acad. Sci. U. S. A.* **100:** 11451–11456

Franc NC, Dimarcq JL, Lagueux M, Hoffmann J & Ezekowitz R a B (1996) Croquemort, a novel drosophila hemocyte/macrophage receptor that recognizes apoptotic cells.

Immunity **4:** 431–443

Franzén O & Björkegren JLM (2020) alona: a web server for single cell RNA-seq analysis. *Bioinformatics***:** 1–3

Goto A, Kadowaki T & Kitagawa Y (2003) Drosophila hemolectin gene is expressed in embryonic and larval hemocytes and its knock down causes bleeding defects. *Dev. Biol.* **264:** 582–591

Gulley MM, Zhang X & Michel K (2013) The roles of serpins in mosquito immunology and physiology. *J. Insect Physiol.* **59:** 138–147

Guo H, Li Y, Zhang M, Li R, Li W, Lou J, Bao Z & Wang Y (2018) Expression of Cathepsin F in response to bacterial challenges in Yesso scallop Patinopecten yessoensis. *Fish Shellfish Immunol.* **80:** 141–147

Haghverdi L, Lun ATL, Morgan MD & Marioni JC (2018) Batch effects in single-cell RNA-sequencing data are corrected by matching mutual nearest neighbors. *Nat. Biotechnol.* **36:** 421–427

Hillyer JF, Schmidt SL & Christensen BM (2003) Rapid phagocytosis and melanization of bacteria and Plasmodium sporozoites by hemocytes of the mosquito Aedes aegypti. *J. Parasitol.* **89:** 62–69

Hillyer JF & Strand MR (2014) Mosquito hemocyte-mediated immune responses. *Curr. Opin. Insect Sci.* **3:** 14–21

Horne MC, Donaldson KL, Goolsby GL, Tran D, Mulheisen M, Hell JW & Wahl AF (1997) Cyclin G2 is up-regulated during growth inhibition and B cell antigen receptor-mediated cell cycle arrest. *J. Biol. Chem.* **272:** 12650–12661

Hurd H, Taylor PJ, Adams D, Underhill a & Eggleston P (2005) Evaluating the costs of mosquito resistance to malaria parasites. *Evolution* **59:** 2560–2572

Iwama R & Ashida M (1986) Biosynthesis of prophenoloxidase in hemocytes of larval hemolymph of the silkworm, Bombyx mori. *Insect Biochem.* **16:** 547–555

Jiang S, Qiu L, Wang L, Jia Z, Lv Z, Wang M, Liu C, Xu J & Song L (2018) Transcriptomic

and quantitative proteomic analyses provide insights into the phagocytic killing of hemocytes in the Oyster Crassostrea gigas. *Front. Immunol.* **9:**

Kanost MR & Jiang H (2015) Clip-domain serine proteases as immune factors in insect hemolymph. *Curr. Opin. Insect Sci.* **11:** 47–55

Kim D, Langmead B & Salzberg SL (2015) HISAT: A fast spliced aligner with low memory requirements. *Nat. Methods* **12:** 357–360

King JG & Hillyer JF (2013) Spatial and temporal in vivo analysis of circulating and sessile immune cells in mosquitoes: hemocyte mitosis following infection. *BMC Biol.* **11:** 55

Kocks C, Cho JH, Nehme N, Ulvila J, Pearson AM, Meister M, Strom C, Conto SL, Hetru C, Stuart LM, Stehle T, Hoffmann JA, Reichhart J-M, Ferrandon D, Rämet M & Ezekowitz RAB (2005) Eater, a Transmembrane Protein Mediating Phagocytosis of Bacterial Pathogens in Drosophila. *Cell* **123:** 335–346

Koranteng F, Cha N, Shin M & Shim J (2020) The Role of Lozenge in Drosophila Hematopoiesis. *Mol. Cells* **43:** 114–120

Krishna S, Yim DG, Lakshmanan V, Tirumalai V, Koh JL, Park JE, Cheong JK, Low JL, Lim MJ, Sze SK, Shivaprasad P, Gulyani A, Raghavan S, Palakodeti D & DasGupta R (2019) Dynamic expression of tRNA-derived small RNAs define cellular states. *EMBO Rep.***:** e47789

Kurucz E, Zettervall C-J, Sinka R, Vilmos P, Pivarcsi A, Ekengren S, Hegedüs Z, Ando I & Hultmark D (2003) Hemese, a hemocyte-specific transmembrane protein, affects the cellular immune response in Drosophila. *Proc. Natl. Acad. Sci. U. S. A.* **100:** 2622–2627

Kwon H, Arends BR & Smith RC (2017) Late-phase immune responses limiting oocyst survival are independent of TEP1 function yet display strain specific differences in Anopheles gambiae. *Parasit. Vectors* **10:** 369

Kwon H & Smith RC (2019) Chemical depletion of phagocytic immune cells in Anopheles gambiae reveals dual roles of mosquito hemocytes in anti- Plasmodium immunity. *Proc. Natl. Acad. Sci.* **116:** 14119–14128

Langfelder P, Zhang B & Horvath S (2008) Defining clusters from a hierarchical cluster tree: The Dynamic Tree Cut package for R. *Bioinformatics* **24:** 719–720

Lavine M & Strand MR (2002) Insect Hemocytes and Their Role in Immunity. *Insect Biochem. Mol. Biol.* **32:** 1295–1309

Leitao AB & Sucena E (2015) Drosophila sessile hemocyte clusters are true hematopoietic tissues that regulate larval blood cell differentiation. *Elife* **2015:** 1–38

Liao Y, Smyth GK & Shi W (2014) FeatureCounts: An efficient general purpose program for assigning sequence reads to genomic features. *Bioinformatics* **30:** 923–930

Lu A, Zhang Q, Zhang J, Yang B, Wu K, Xie W, Luan YX & Ling E (2014) Insect prophenoloxidase: The view beyond immunity. *Front. Physiol.* **5 JUL:** 1–15

Manaka J, Kuraishi T, Shiratsuchi A, Nakai Y, Higashida H, Henson P & Nakanishi Y (2004) Draper-mediated and phosphatidylserine-independent phagocytosis of apoptotic cells by Drosophila hemocytes/macrophages. *J. Biol. Chem.* **279:** 48466–48476

Martinek N, Shahab J, Saathoff M & Ringuette M (2011) Haemocyte-derived SPARC is required for collagen-IV-dependent stability of basal laminae in Drosophila embryos. *J. Cell Sci.* **124:** 670–670

Martínez-Gac L, Marqués M, García Z, Campanero MR & Carrera AC (2004) Control of Cyclin G2 mRNA Expression by Forkhead Transcription Factors: Novel Mechanism for Cell Cycle Control by Phosphoinositide 3-Kinase and Forkhead. *Mol. Cell. Biol.* **24:** 2181–2189

Mendes AM, Awono-Ambene PH, Nsango SE, Cohuet A, Fontenille D, Kafatos FC, Christophides GK, Morlais I & Vlachou D (2011) Infection intensity-dependent responses of Anopheles gambiae to the African malaria parasite Plasmodium falciparum. *Infect. Immun.* **79:** 4708–4715

Midega J, Blight J, Lombardo F, Povelones M, Kafatos F & Christophides GK (2013) Discovery and characterization of two Nimrod superfamily members in Anopheles gambiae. *Pathog. Glob. Health* **107:** 463–74

Miller M, Chen A, Gobert V, Augé B, Beau M, Burlet-Schiltz O, Haenlin M & Waltzer L (2017) Control of RUNX-induced repression of Notch signaling by MLF and its partner DnaJ-1 during Drosophila hematopoiesis. *PLoS Genet.* **13:** 1–28

Mortazavi A, Williams BA, McCue K, Schaeffer L & Wold B (2008) Mapping and quantifying mammalian transcriptomes by RNA-Seq. *Nat. Methods* **5:** 621–628

Packer JS, Zhu Q, Huynh C, Sivaramakrishnan P, Preston E, Dueck H, Stefanik D, Tan K, Trapnell C, Kim J, Waterston RH & Murray JI (2019) A lineage-resolved molecular atlas of C. Elegans embryogenesis at single-cell resolution. *Science* **365:** eaax1971

Papalexi E & Satija R (2017) Single-cell RNA sequencing to explore immune cell heterogeneity. *Nat. Rev. Immunol.* **18**: 35–45

Picelli S, Björklund ÅK, Faridani OR, Sagasser S, Winberg G & Sandberg R (2013) Smart-seq2 for sensitive full-length transcriptome profiling in single cells. *Nat. Methods* **10:** 1096–1100

Picelli S, Faridani OR, Björklund ÅK, Winberg G, Sagasser S & Sandberg R (2014) Full-length RNA-seq from single cells using Smart-seq2. *Nat. Protoc.* **9:** 171–181

Pinto SB, Lombardo F, Koutsos AC, Waterhouse RM, McKay K, An C, Ramakrishnan C, Kafatos FC & Michel K (2009) Discovery of Plasmodium modulators by genome-wide analysis of circulating hemocytes in Anopheles gambiae. *Proc. Natl. Acad. Sci. U. S. A.* **106:** 21270–21275

Pondeville E, Puchot N, Parvy JP, Carissimo G, Poidevin M, Waterhouse RM, Marois E & Bourgouin C (2020) Hemocyte-targeted gene expression in the female malaria mosquito using the hemolectin promoter from Drosophila. *Insect Biochem. Mol. Biol.* **120:** 103339

Proserpio V & Mahata B (2016) Single-cell technologies to study the immune system. *Immunology* **147:** 133–140

Qiu X, Hill A, Packer J, Lin D, Ma YA & Trapnell C (2017a) Single-cell mRNA quantification and differential analysis with Census. *Nat. Methods* **14:** 309–315

Qiu X, Mao Q, Tang Y, Wang L, Chawla R, Pliner HA & Trapnell C (2017b) Reversed graph embedding resolves complex single-cell trajectories. *Nat. Methods* **14:** 979–982

Raddi G, Barletta ABF, Efremova M, Ramirez JL, Cantera R, Teichmann SA, Barillas-Mury C & Billker O (2020) Mosquito cellular immunity at single-cell resolution. *bioRxiv***:** 2020.04.08.032508

Rak R, Polonsky M, Eizenberg I, Dahan O, Friedman N & Pilpel YT (2020) Dynamic changes in tRNA modifications and abundance during T-cell activation. *bioRxiv***:** 2020.03.14.991901

Ramirez JL, de Almeida Oliveira G, Calvo E, Dalli J, Colas R a., Serhan CN, Ribeiro JM & Barillas-Mury C (2015) A mosquito lipoxin/lipocalin complex mediates innate immune priming in Anopheles gambiae. *Nat. Commun.* **6:** 7403

Ramirez JL, Garver LS, Brayner FA, Alves LC, Rodrigues J, Molina-Cruz A & Barillas-Mury C (2014) The role of hemocytes in anopheles gambiae antiplasmodial immunity. *J. Innate Immun.* **6:** 119–128

Ranford-Cartwright LC, McGeechan S, Inch D, Smart G, Richterová L & Mwangi JM (2016) Characterisation of Species and Diversity of Anopheles gambiae Keele Colony. *PLoS One* **11:** e0168999

Reynolds RA, Kwon H & Smith RC (2020) 20-Hydroxyecdysone Primes Innate Immune Responses That Limit Bacterial and Malarial Parasite Survival in Anopheles gambiae. *mSphere* **5:** e00983-19

Ribeiro C & Brehélin M (2006) Insect haemocytes: What type of cell is that? *J. Insect Physiol.* **52:** 417–429

Rodrigues J, Brayner FA, Alves LC, Dixit R & Barillas-Mury C (2010) Hemocyte differentiation mediates innate immune memory in Anopheles gambiae mosquitoes. *Science* **329:** 1353–1355

Severo MS, Landry JJMM, Lindquist RL, Goosmann C, Brinkmann V, Collier P, Hauser AE, Benes V, Henriksson J, Teichmann SA & Levashina EA (2018) Unbiased

classification of mosquito blood cells by single-cell genomics and high-content imaging. *Proc. Natl. Acad. Sci. U. S. A.*: 201803062

Smith RC, Barillas-Mury C & Jacobs-Lorena M (2015) Hemocyte differentiation mediates the mosquito late-phase immune response against Plasmodium in Anopheles gambiae. *Proc. Natl. Acad. Sci.* **112:** E3412-20

Smith RC, King JG, Tao D, Tomescu O, Brando C, Thallinger GG, Dinglasan RR, Zeleznik OA, Brando C, Thallinger GG & Dinglasan RR (2016) Molecular profiling of phagocytic immune cells in Anopheles gambiae reveals integral roles for hemocytes in mosquito innate immunity. *Mol. Cell. proteomics* **15:** 3373–3387

Stofanko M, So YK & Badenhorst P (2008) A misexpression screen to identify regulators of drosophila larval hemocyte development. *Genetics* **180:** 253–267

Stuart T & Satija R (2019) Integrative single-cell analysis. *Nat. Rev. Genet.* **20:** 257–272

Szabo PA, Levitin HM, Miron M, Snyder ME, Senda T, Yuan J, Cheng YL, Bush EC, Dogra P, Thapa P, Farber DL & Sims PA (2019) Single-cell transcriptomics of human T cells reveals tissue and activation signatures in health and disease. *Nat. Commun.* **10:** 4706

Tattikota SG, Hu Y, Liu Y, Cho B, Barrera V, Steinbaugh M, Yoon S-H, Comjean A, Li F, Dervis F, Hung R-J, Nam J-W, Sui SH, Shim J & Perrimon N (2020) A single-cell survey of Drosophila blood. *Elife* **9:** e54818

Terriente-Felix A, Li J, Collins S, Mulligan A, Reekie I, Bernard F, Krejci A & Bray S (2013) Notch cooperates with Lozenge/Runx to lock haemocytes into a differentiation programme. *Dev.* **140:** 926–937

Torrent M, Chalancon G, De Groot NS, Wuster A & Madan Babu M (2018) Cells alter their tRNA abundance to selectively regulate protein synthesis during stress conditions. *Sci. Signal.* **11:** 1–10

Trapnell C, Cacchiarelli D, Grimsby J, Pokharel P, Li S, Morse M, Lennon NJ, Livak KJ, Mikkelsen TS & Rinn JL (2014) The dynamics and regulators of cell fate decisions are revealed by pseudotemporal ordering of single cells. *Nat. Biotechnol.* **32:** 381–

386

Tryselius Y & Hultmark D (1997) Cysteine proteinase 1 (CP1), a cathepsin L-like enzyme expressed in the Drosophila melanogaster haemocyte cell line mbn-2. *Insect Mol. Biol.* **6:** 173–181

Waltzer L, Ferjoux G, Bataillé L & Haenlin M (2003) Cooperation between the GATA and RUNX factors Serpent and Lozenge during Drosophila hematopoiesis. *EMBO J.* **22:** 6516–6525

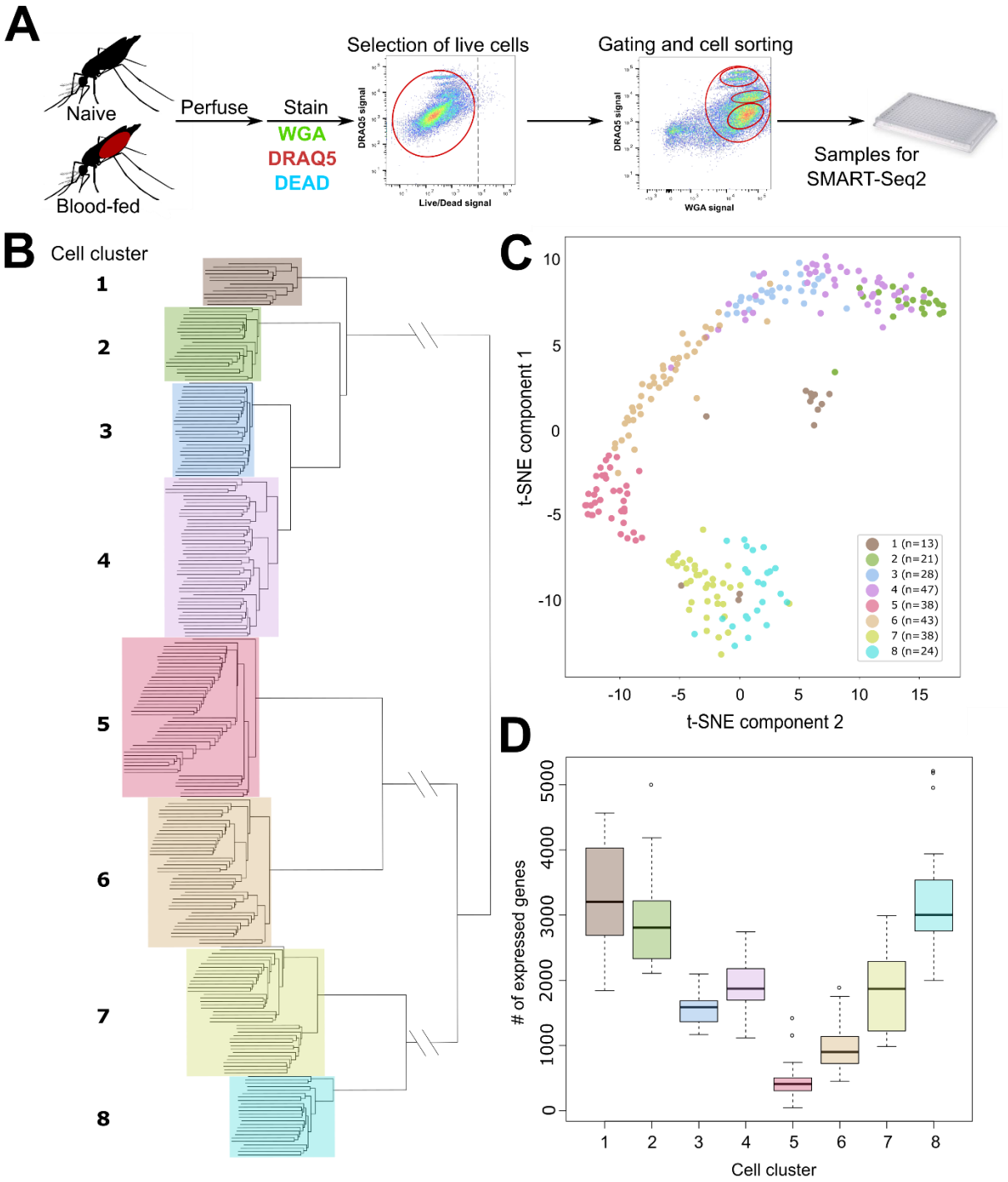

Figure 1. **scRNA-seq of *An.gambiae* immune cells. (A)** Graphical overview of the isolation of mosquito immune cells from naïve and blood-fed mosquitoes. Following perfusion, cells were stained to enable processing by fluorescent activated cell sorting (FACS) and isolation for scRNA-seq. Resulting immune cells data were separated into 8

cell clusters based on hierarchical clustering analysis **(B)** and visualized using a t-Distributed Stochastic Neighbor Embedding (t-SNE) plot **(C)**. The number of expressed genes per cluster are displayed as a boxplot **(D)**.

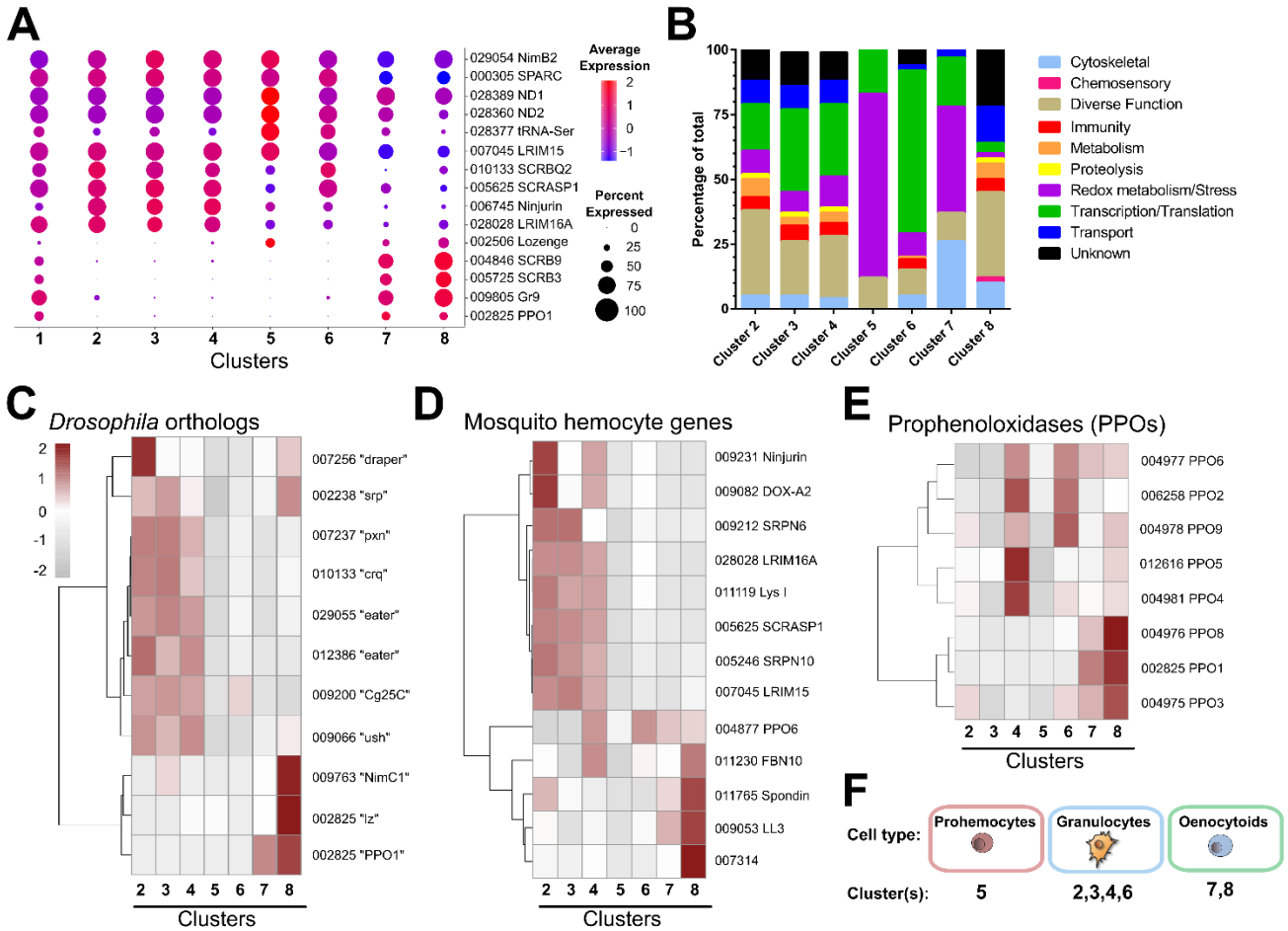

Figure 2. **Comparitive analysis of mosquito immune cells. (A)** Marker gene expression displayed by dot plot across cell clusters. **(B)** Gene ontology (GO) analysis of genes expressed in >80% cells within each respective cluster. Heat maps of candidate genes to *Drosophila* hemocyte orthologs **(C)**, described mosquito hemocyte genes **(D)**, or *An. gambiae* prophenoloxidases (PPOs) **(E)** to enable the characterization of immune cells form each cell cluster. **(F)** From these analysis, immune cells of each cluster were assigned to tentative cell types (prohemocytes, granulocytes, oenocytoids).

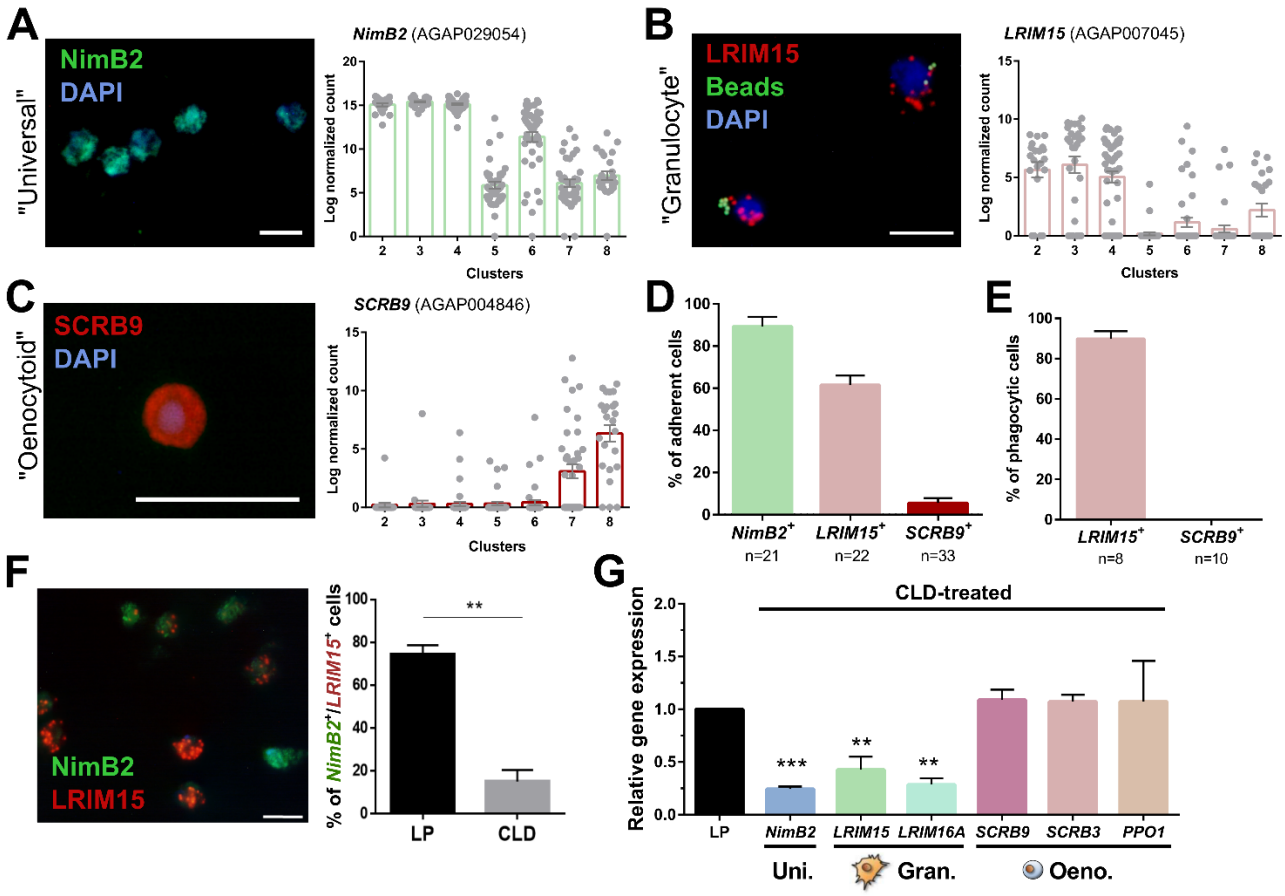

Figure 3. **Definition of mosquito immnue cell sub-types.** RNA-FISH and gene expression profiles across cell clusters for the "universal" marker, *NimB2* **(A)**, the "granulocyte" marker, *LRIM15* **(B)**, and "oenocytoid" marker, *SCRB9* **(C)**. The percentage of adherent cells following fixation was evaluated for each of the respective *NimB2*, *LRIM15*, and *SCRB9* markers in four or more independent replicates **(D)**. To determine the phagocytic abilty of granulocytes and oeonocytoids, the uptake of fluorescent beads was evaluated in either LRIM15^{+} or SCRB9^{+} cells in two independent replicates **(E)**. The phagocytic ability of LRIM15^{+} cells was further validated by examining the abundance of NimB2^{+}/LRIM15^{+} cells by RNA-FISH following perfusion after treatment with control (LP)- or clodronate (CLD) liposomes that deplete phagocytic cells **(F)**. Data were analyzed using a Mann–Whitney test using GraphPad Prism 6.0. Bars represent mean ± SE of two independent replicates. Additional validation of clodronate (CLD) depletion of phagocytic cells was performed by qRT-PCR using primers for universal (uni.), granulocyte (gran.), and oenocytoid (oeno.) cell markers. Data were analyzed using an unpaired t test to

determine differences in relative gene expression between LP and CLD treatments. Bars represent mean ± SE of three independent replications (**G**). Asterisks denote significance (**$P < 0.01$, ***$P < 0.001$). Scale bar, 10 µm.

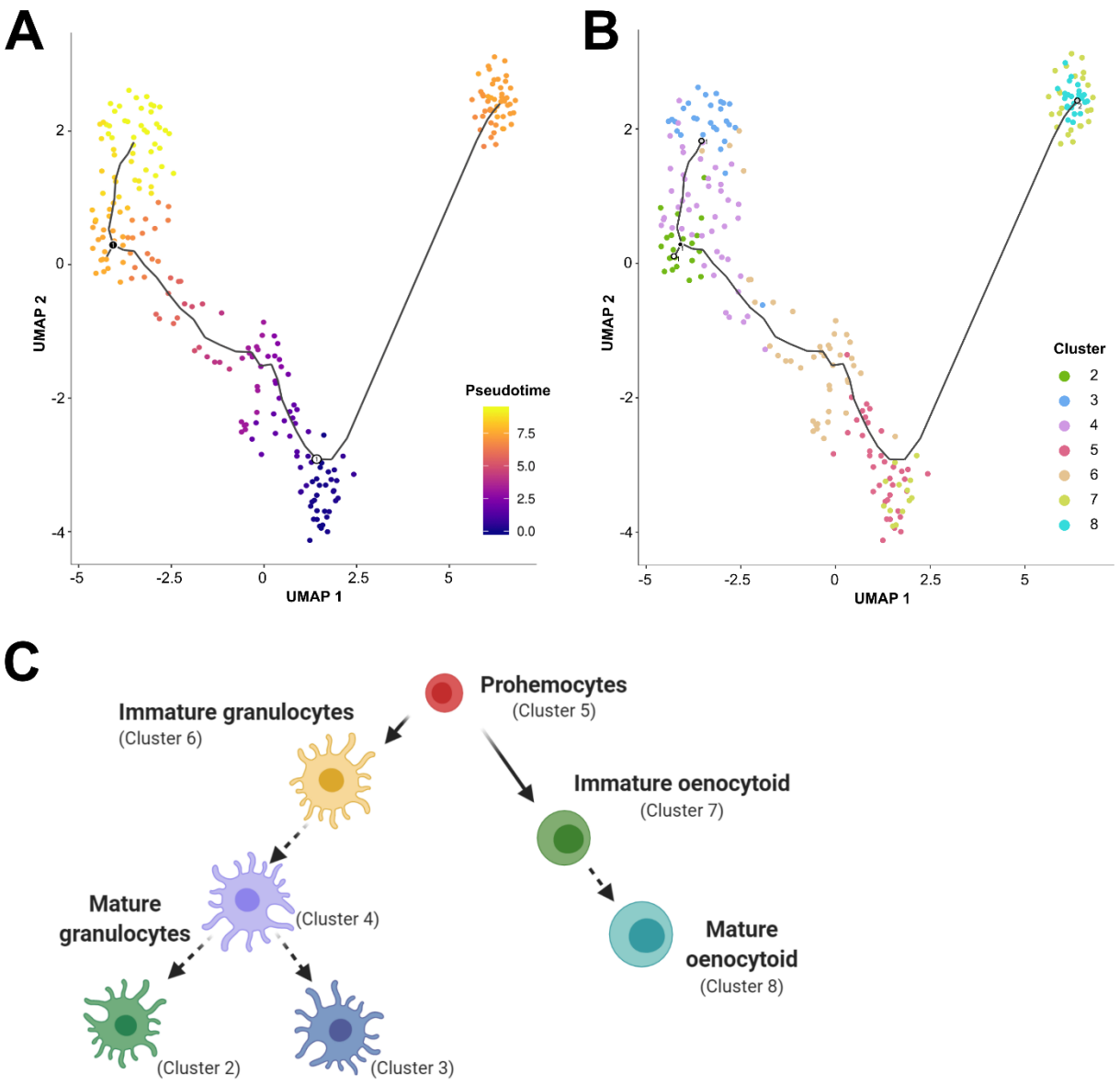

Figure 4. **Lineage analysis of mosquito immune cells.** Using Monocle3, mosquito immune cells were visualized by UMAP to reveal two distinct lineages in pseudotime **(A)** or to display cells of each respective immune cell cluster **(B)**. From the lineage analysis and in combination with other functional assays, our data support the following model of immune cell development and differentiation where prohemocytes serve as precursors for the granulocyte and oenocytoid lineages **(C)**. Each cell type is labeled with the correposnding cell cluster described in our anlaysis.

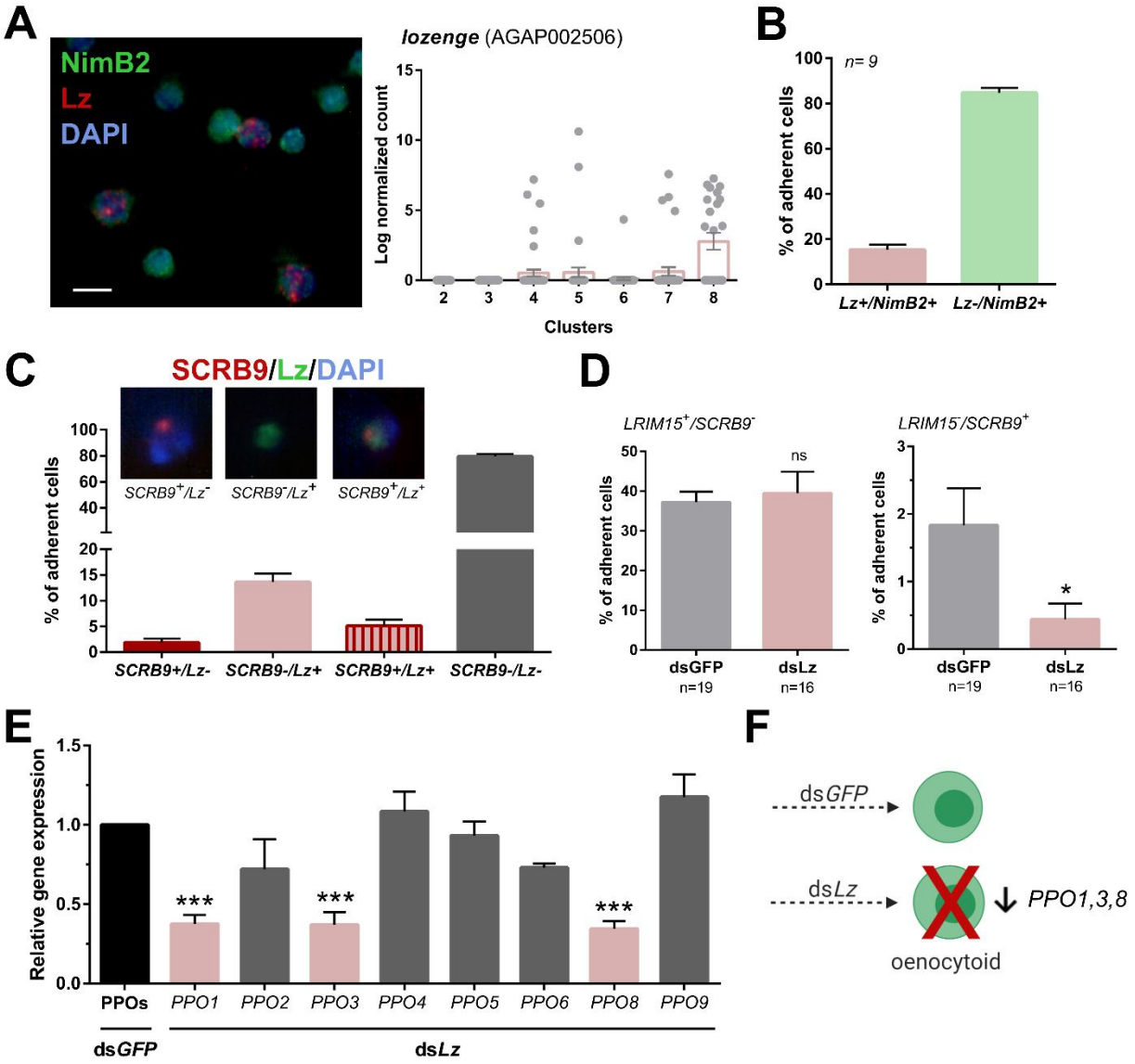

Figure 5. Lozenge promotes oenocytoid differention. RNA-FISH and gene expression profiles across cell clusters for *lozenge (Lz)* **(A)**. Scale bar, 10 µm. The percentage of adherent *Lz*$^{+}$*/NimB2*$^{+}$ or *Lz*$^{-}$*/NimB2*$^{+}$ cells were examined in naïve adult female mosquitoes to estimate cell abundance **(B)**. Data were collected from two independent experiments. To more closely examine the population of *Lz*+ cells, RNA-FISH experiments were performed double staining for *Lz* and the oenocytoid marker, *SCRB9* **(C)**. The percentage of fixed cells positive for one, both, or neither marker is displayed with representative images. Data are summarized from two independent experiments. To

determine the effects of Lz on immune cell populations, the abundance of *LRIM15*$^{+}$*/SCRB9*$^{-}$ (granulocyte) and *LRIM15*$^{-}$*/SCRB9*$^{+}$ (oenocytoid) cells were evealuated by RNA-FISH after *GFP* (control)- or *Lz*-silencing **(D)**. Data represent the mean ± SE of three independent replicates. Significance is denoted by an asterisk (*$P < 0.05$); ns, not significant. Since Lz expression has previously been associated with prophenoloxidase (PPO) expression, the expression of all 8 genes identified in our scRNA-seq analysis were examined by qRT-PCR in GFP (control) - *Lz*-silenced mosquitoes **(E)**. Data represent the mean ± SE of three or more independent replicates and were analyzed by a One-way ANOVA and Holm-Sidak's multiple comparison test using GraphPad Prism 6.0. Asterisks denote significance (***$P < 0.001$). **(F)** Summary of *Lz*-silencing experiments which display a reduction in oenocytoid numbers and a specific sub-set of PPO gene expression which support that Lz is integral to the differentiation of the mosquito oenocytoid lineage.